Research Journal of Material Sciences ISSN 2320–6055
Vol. **11(2),** 1-5, August **(2023)** *Res. J. Material Sci.*

The effects of doping additives on the conductivities of Poly(3,4-ethylenedioxythiophene)

V.S. Bhavale[2], A.B. Chourasia[1,2]* and D.S. Kelkar[3]
[1]Electronic Science Dept., H.P.T. Arts and R.Y.K. Science College, Nashik-422 005, India
[2]Department of Physics H.P.T. Arts and R.Y.K. Science College, Nasik-422 005, India
[3]Department of Physics, Govt. Institute of Science, Nagpur, India
abchourasiansk@rediffmail.com

Available online at: www.isca.in, www.isca.me
Received 23th July 2021, revised 29th May 2023, accepted 16th June 2023

Abstract

The polymer Poly (3,4-ethylenedoixythiophene) (PEDOT) underwent a chemical synthesis process and was subsequently doped with $FeCl_3$ and Camphor Sulfonic Acid (CSA). The utilization of FTIR analysis verified the successful synthesis of PEDOT, as well as the desired doping with $FeCl_3$ and CSA. The crystal structure of the samples was analysed using XRD, revealing modifications following doping. Additionally, the XRD results allowed for the calculation of sample crystallinity, which increased after doping with $FeCl_3$, but decreased after doping with CSA. Using the four-probe method, electrical conductivity (σ) measurements were obtained, showing a significant increase in conductivity after doping with both $FeCl_3$ and CSA, with the undoped sample having a conductivity of $3.41X10^{-3}$S/cm. A plot of Log σ versus 1/T was created, revealing that the undoped PEDOT had metallic characteristics above 308°K, while both doped samples displayed semiconducting behaviour in the temperature range from ambient to 383° K. An apparatus similar to Lee's method was used for measuring the thermal conductivity, which revealed that all samples exhibited comparatively small thermal conductivity values. However, these values were found to increase upon doping and with a rise in temperature.

Keywords: Poly(3,4-ethylenedoixythiophene) (PEDOT), Lee's Method.

Introduction

A polymer is a type of large molecule composed of repeating structural units that are linked together by covalent bonds. The term "large molecule" typically refers to those with a molecular weight of 1000 or more or containing 100 or more structural units. A structural unit is a group of atoms that are covalently bonded together in a specific arrangement. Unlike solids and liquids in which repeating units (such as ions, atoms, or molecules) are held together by ionic bonds, metallic bonds, hydrogen bonds, dipole interactions, or vander Waals forces, polymers are characterized by the covalent bonds that link their structural units together.

Over the past three decades, significant research efforts have been dedicated to the exploration of novel category of materials known as organic conducting polymers. Conducting polymers, including polyaniline, polypyrrol, and polythiophene, have found a vast range of applications in electronics and other fields, from everyday household items to space technology. Among these conducting polymers, PEDOT boasts several advantageous properties. One of its most promising features is the ability to electrochemically synthesize films with a low redox potential and exceptional stability in their doped state[1]. Due to these properties, PEDOT is an excellent candidate for various electronic applications, such as capacitors[2], electroluminescent lamps[3], electronic devices[4], sensors[5], photovoltaic cells[1], and OLEDs[1]. PEDOT has proven to be a highly effective material for electronic devices[4]. To be suitable for electronic applications, a material must exhibit high DC electrical conductivity and low thermal conductivity.

Methodology

Sample preparation: In a previous publication[6,7], methods were described for synthesizing undoped and re-doped PEDOT samples using various dopants, including $FeCl_3$ and Camphor Sulfonic Acid (CSA).

Characterization: The FTIR spectra were obtained using a Shimadzu (Japan) FTIR-8400S spectrophotometer within the interval of $4000cm^{-1}$ to $400cm^{-1}$. UV-2450 UV-VIS Spectrophotometer was used to investigate the optical properties in the wavelength range of 250-650 nm. The XRD patterns of all samples were recorded between $2\theta = 5°$ to 50° to study the modifications after doping PEDOT with $FeCl_3$ and CSA. The electrical conductivity (σ) was determined using the four-probe method by calculating the inverse of the measured electrical resistivity. Thermal conductivity observations for different temperatures were conducted utilizing an instrument designed in-house.

Thermal Conductivity Instrument: The laboratory-built thermal conductivity measurement instrument shares similarities with Lee's Method. However, Lee's method involves passing steam through a hollow brass cylinder, limiting measurements

to the boiling point of water. In contrast, the newly designed instrument employs an electrical heater (in place of the steam chamber) that can be adjusted to various temperatures range from ambient to 250°C. Once the lower disc reaches a steady state, the set temperature can be maintained for extended periods. Thus, the newly designed instrument allows for thermal conductivity measurements at various temperatures within the stated range. In contrast to Lee's method, where the experiment is conducted in natural atmospheric conditions, the newly designed instrument allows for experimentation in a vacuum chamber. This eliminates the possibility of oxidation of the polymeric material due to heat and reduces heat loss due to the atmosphere. The upper- and lower-disc temperatures are measured using PT-100 sensors, and the measured temperatures are displayed digitally with an accuracy of 0.1°C.

To prevent Infrared (IR) radiation from interfering with the thermal conductivity measurements, aluminium foil is utilized as it is an electrically conductive material that can effectively block IR. The effectiveness of blocking IR is higher for materials with higher conductivity. Aluminium foil has the ability to block infrared radiation in both the high and low ranges. Plastics are IR-transparent, meaning they allow infrared radiation to pass through them. In contrast, glass is selective in its IR transmission, blocking low-frequency IR while permitting high-frequency IR to pass through, resulting in the heat from the sun effortlessly enter a greenhouse. However, when the objects absorb energy by the objects within the greenhouse and converted into low-frequency heat, it becomes trapped within the greenhouse.

Results and Discussion

FTIR Spectroscopy: These FT-IR bonds were examined to assess any structural changes in the PEDOT polymer resulting from doping with $FeCl_3$ and CSA. Prior to doping, the polymer was undoped using hydrazine, and an IR spectrum was obtained. The C-S bond vibration mode in the thiophene ring was found to correspond to an absorption band at 840.99cm^{-1}. Additionally, strong absorption bands at 1060.88cm^{-1} and 1193.98cm^{-1} were attributed to the characteristic C-O bond, while the C=C bond was identified at 1340.57cm-1. The vibrational band observed at 1500.67cm^{-1} was linked with the ring vibrational mode of the thiophene ring, and bands between 2850-3000cm^{-1} confirmed that the synthesized polymer was PEDOT and coupled at the α-α' position[8,9].

$FeCl_3$ was used to dope PEDOT for duration of 5 hours, resulting in the appearance of a new band at 570.93cm^{-1}. Bands within the 550-780cm^{-1} range were attributed to the presence of C-Cl bonds, which were not observed in undoped PEDOT[10]. The shift from 918.15cm^{-1} in undoped PEDOT to 920.05cm^{-1} in $FeCl_3$ doped PEDOT indicated deformation of the ethylenedioxy ring following doping. The vibration band observed at 840.99 cm^{-1} in undoped PEDOT shifted to 835.18 cm^{-1} after doping with $FeCl_3$, indicating attachment of Fe to the S in the thiophene ring. Additionally, the very strong bonds detected at 1060.88cm^{-1} and 1193.98cm^{-1} in undoped PEDOT, which corresponded to C-O bonds, shifted to 1053.13cm^{-1} and 1207.44cm^{-1} in $FeCl_3$ doped PEDOT. Meanwhile, undoped PEDOT was also doped using CSA for a duration of 5 hours, resulting in the appearance of new bands at 1091.71 cm^{-1} and 1382.96cm^{-1}, which were attributed to the S-Aryl and CH_3-S bands, respectively. The ring vibrational mode of the thiophene ring (1350-1500cm^{-1}) at 1500.67cm^{-1} in undoped PEDOT shifted to 1521.84cm^{-1}, corresponding to the CH_3 group of the CSA moiety forming either bonds or an interface with the thiophene ring.

XRD Analysis: The X-ray diffraction (XRD) analysis, shown in Figure-1, was used to investigate the phase, structure, and crystallinity of the synthesized material. Table-1 summarizes the results of the XRD analysis, which is performed using 2θ angle. The presence of the dopant and the S atom of the thiophene ring is confirmed by the presence of peaks between 5-7° in all three samples[11]. Additionally, the XRD pattern shows a broad peak around 2θ= 25-27° for all samples, indicating that the particle size of the samples is in the nanoscale range[12,13]. PEDOT undergoes structural modification and the peak shifts towards the right after doping with $FeCl_3$ and CSA. The degree of crystallinity in undoped and doped PEDOT samples was determined with an error of 5-8% using the analysis described in Manjunath et al[14]. It was found that the degree of crystallinity increased after doping with $FeCl_3$, resulting in an amorphous nature. Conversely, doping with CSA resulted in a disturbance of the regular arrangement of undoped PEDOT due to the presence of a large, heavy molecule, leading to a decrease in crystallinity.

Table-1: Crystallinity and Peak positions from XRD of samples.

Samples	Peak position at 2Θ	Crystallinity in %
Hydrazine Undoped PEDOT	a) 7.14	33
	b) 12.77	
	c) 26.60	
	d) 33.86	
	e) 36.98	
	a) 7.29	
5 hrs $FeCl_3$ doped	b) 12.77	47
	c) 26.88	
	d) 34.12	
	e) 38.55	
	a) 6.74	
5 hrs CSA Doped	b) 12.15	25
	c) 26.96	
	d) 33.42	
	e) 37.70	

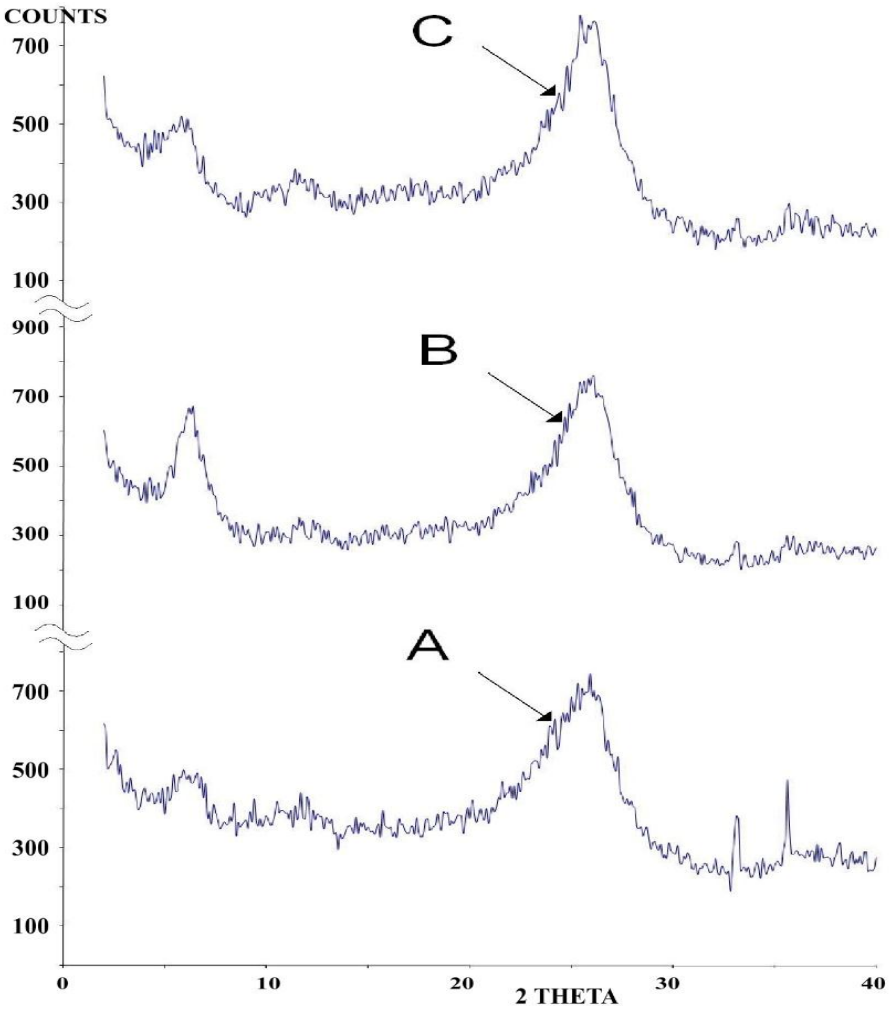

Figure-1: XRD pattern of (A) 5 hrs $FeCl_3$ (B) 5 hrs CSA (C) Hydrazine undoped PEDOT.

UV- visible Analysis: The UV-visible absorption results of Hydrazine undoped, 5hrs $FeCl_3$, and 5 hrs CSA doped samples in the range of 250-650 nm are presented in Figure-2, revealing their optical properties. In the Hydrazine undoped sample, a distinct absorption peak is observed at 299nm, whereas in the 5hrs $FeCl_3$ doped sample, the peak is observed at 304 nm. For the 5hrs CSA doped sample, the absorption peak is observed at 306 nm indicating maximum energy absorption at these wavelengths. The optical band gap energy of the samples is calculated using the formula $E=hc/\lambda$, where h is plank's constant, and c is the velocity of light at the peak wavelength. At the peak wavelength, the undoped sample displays a band gap energy value of 4.15eV, while the $FeCl_3$ doped and CSA doped samples exhibit band gap energy values of 4.08eV and 4.05eV, respectively. The findings indicate that introducing $FeCl_3$ and CSA as dopants causes a reduction in the optical band gap energy. Specifically, the sample doped with CSA exhibits the least optical band gap energy compared to the other samples examined.

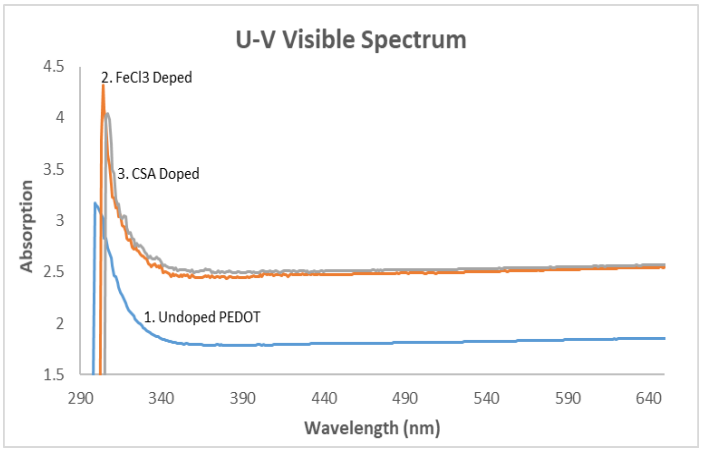

Figure-2: UV-Visible results of 1. Hydrazine, 2. 5hrs $FeCl_3$, 3. 5 hrs CSA doped.

Electrical Conductivity Measurements: The Four-point methodology was employed to measure the dc electrical

conductivity (σ) of undoped PEDOT as well as PEDOT doped with $FeCl_3$ and CSA. Measurements were taken within the temperature range of 300-400 K. The electrical conductivity values of Hydrazine undoped PEDOT, 5 hrs $FeCl_3$, and 5 hrs CSA doped PEDOT were determined by measuring their (dc) conductivity at room temperature (302K). The resulting conductivity values for each sample were $3.42X10^{-3}$S/cm, $4.66X10^{-1}$ S/cm, and $6.13X10^{-1}$ S/cm, respectively. The increase in conductivity by two orders of magnitude suggests that doping has significantly enhanced the conductivity of the samples. The conductivity versus reciprocal temperature (1/T) plot for hydrazine undoped and all doped samples is illustrated in Figure-3. The plot demonstrates that conductivity of undoped PEDOT initially increases and then slightly decreases, indicating the metallic nature of samples within the aforementioned temperature range. On the other hand, for $FeCl_3$ and CSA doped PEDOT, conductivity increases with increasing temperature, affirming their semiconductor behaviour.

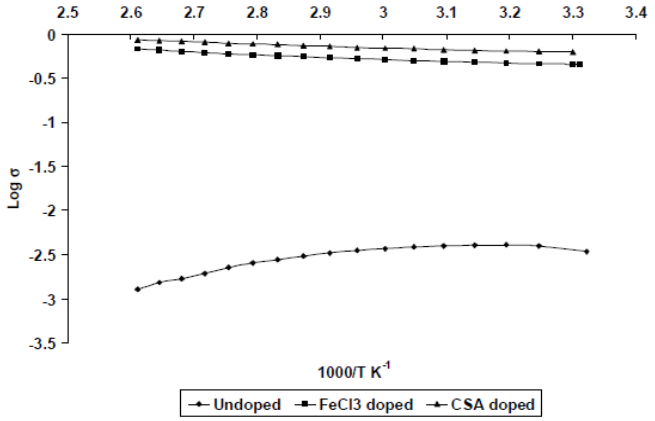

Figure-3: Log *σ vs.* 1/*T* for Hydrazine undoped and doped samples.

Thermal Conductivity Measurement: We used the instrument described in section 2.3 to measure the thermal conductivity of Hydrazine undoped PEDOT, $FeCl_3$, and CSA doped. The observations were taken using the FOX-50 heat flow meter at a temperature of 343 K, and the results are presented in table 2. To obtain these results, we placed the samples in the sample holder and conducted observations at different temperatures ranging from 300 K to 425 K, with 5 K increments between each measurement. The thermal conductivity at each temperature was calculated using the formula

$$K = \frac{ms\left(\frac{d\theta}{dt}\right) at\ \theta 2}{\prod r^2[\frac{\theta 1 - \theta 2}{d}]}$$

In the given equation, Θ1 and Θ2 represent the temperature of the upper and lower plates, respectively. The variables K, m, s, d, and r stand for the coefficient of thermal conductivity, mass of the upper plate, specific heat of the disc material, thickness of the pallet, and radius of the pallet, respectively.

Table-2: Thermal Conductivity using FOX-50 heat flow meter (W/mK).

Samples	343K
Hydrazine undoped	0.08525
5hrs $FeCl_3$ doped	0.08236
5hrs CSA doped	0.08261

Thermal conductivity is determined by the number of free electrons and photons in a material. At room temperature, heat transfer in undoped PEDOT occurs primarily through the motion of photons. As the temperature increases, the thermal conductivity of undoped PEDOT also increases, likely due to changes in the number and/or orientation of photons. Doping the undoped sample with $FeCl_3$ and CSA results in a hundredfold increase in electrical conductivity. This increase in electrical conductivity may be attributed to an increase in the number of charge carriers, an increase in the mobility of free charge carriers, or both.

The present study suggests that the increase in electrical conductivity by a factor of hundred after doping with $FeCl_3$ and CSA may be due to an increase in the number of free electrons. However, this increase in the number of electrons could have a negative impact on thermal conductivity as it could potentially disrupt the motion of photons. The rise in the quantity of electrons could create obstacles that impede the transfer of heat from one point to another via photons. Therefore, even though the number of electrons increases after doping, the hydrazine undoped PEDOT exhibits a lower thermal conductivity as compared to other samples.

Table-3: Thermal Conductivity using newly designed instrument (W/mK).

Samples	Conductivity at different temperatures in (W/mK)				
	300K	323K	343K	373K	423K
Hydrazine undoped	0.0092	0.03746	0.0406	0.0577	0.0880
5hrs $FeCl_3$ doped	0.0093	0.03832	0.0420	0.0602	0.0935
5 hrs CSA doped	0.0093	0.03833	0.0418	0.0598	0.0925

Both phonons and free electrons contribute to the heat transport in a material, thereby influencing its thermal conductivity. In this study, although the electrical conductivity of PEDOT increases after doping with $FeCl_3$ and CSA due to the rise in both the quantity and mobility of electrons at elevated temperatures, the values of thermal conductivity of the doped samples remain nearly constant at higher temperatures. This suggests that phonons may not be assisting thermal conductivity and may also be hindering the electrons from carrying heat from one point to another. Additionally, the mobility of photons may have increased with the temperature rise from 300K to 343K, leading to an increase in thermal conductivity in both doped samples. Although exposed to elevated temperatures, the thermal conductivity values of the doped samples persist to exhibit lesser values than the $FeCl_3$ doped sample at 423K.

Conclusion

$FeCl_3$ and CSA are effective dopants for enhancing the electrical conductivity of poly(3,4-ethylenedioxythiophene) PEDOT, with conductivity values increasing by a factor of one hundred. PEDOT can undergo structural modifications upon forming a complex with both dopants, leading to alterations in its crystal structure, as both are capable of binding with it. Apart from that, the doping process leads to a decrease in the optical band gap energy. The X-ray diffraction (XRD) pattern of the prepared samples exhibits broad peaks in the range of 20˚-30˚ angles, confirming their particle size falls within the nanoscale range. Notably, the 5 hrs doped CSA sample displays the minimum optical band gap energy in comparison to all the other samples. While hydrazine undoped PEDOT displays a metallic nature above 308K, both doped samples exhibit a semiconducting nature in the interval of 303 to 383K. Additionally, undoped PEDOT exhibits a relatively low thermal conductivity, which shows an increase upon doping and also with an increase in temperature.

Acknowledgement

We would like to express our gratitude to the Principal of H.P.T. Arts and R.Y.K. Science College, Nashik, V.N. Suryavanshi, for providing financial assistance to conduct this study and the access granted to the research facilities to synthesize the polymer.

References

1. Zhan, L., Song, Z., Zhang, J., Tang, J., Zhan, H., Zhou, Y., & Zhan, C. (2008). PEDOT: Cathode active material with high specific capacity in novel electrolyte system. *Electrochimica Acta*, 53(28), 8319-8323.

2. Wang, Y., Jia, W., Strout, T., Ding, Y., & Lei, Y. (2009). Preparation, characterization and sensitive gas sensing of conductive core-sheath TiO2-PEDOT nanocables. *Sensors*, 9(9), 6752-6763.

3. Louwet, F., Groenendaal, L., Dhaen, J., Manca, J., Van Luppen, J., Verdonck, E., & Leenders, L. (2003). PEDOT/PSS: synthesis, characterization, properties and applications. *Synthetic Metals*, 135(1), 115-118.

4. Groenendaal, L., Zotti, G., Aubert, P. H., Waybright, S. M., & Reynolds, J. R. (2003). Electrochemistry of poly (3, 4-alkylenedioxythiophene) derivatives. *Advanced Materials*, 15(11), 855-879.

5. Bashir, T., Ali, M., Cho, S. W., Persson, N. K., & Skrifvars, M. (2013). OCVD polymerization of PEDOT: effect of pre-treatment steps on PEDOT-coated conductive fibers and a morphological study of PEDOT distribution on textile yarns. *Polymers for advanced technologies*, 24(2), 210-219.

6. Bashir, T., Ali, M., Cho, S. W., Persson, N. K., & Skrifvars, M. (2013). OCVD polymerization of PEDOT: effect of pre-treatment steps on PEDOT-coated conductive fibers and a morphological study of PEDOT distribution on textile yarns. *Polymers for advanced technologies*, 24(2), 210-219.

7. Chourasia, A. B. (2016). Thermal Conductivity of Poly. *Research Journal of Material Sciences*, 4(6), 1-5.

8. Meng, H., Perepichka, D. F., Bendikov, M., Wudl, F., Pan, G. Z., Yu, W., ... & Brown, S. (2003). Solid-state synthesis of a conducting polythiophene via an unprecedented heterocyclic coupling reaction. *Journal of the American Chemical Society*, 125(49), 15151-15162.

9. Yamamoto, T., & Abla, M. (1999). Synthesis of non-doped poly (3, 4-ethylenedioxythiophene) and its spectroscopic data. *Synthetic Metals*, 100(2), 237-239.

10. Donald, L., Gary M.. Lampman, & Kriz, G. S. (1996). Introduction to spectroscopy: A guide for students of organic chemistry. Saunders college publishing.

11. Bhadra, S., & Khastgir, D. (2008). Determination of crystal structure of polyaniline and substituted polyanilines through powder X-ray diffraction analysis. *Polymer Testing*, 27(7), 851-857.

12. Hebbar, K. R. (2007). Basics of X-ray diffraction and its applications. IK International Publishing House Pvt. Limited.

13. Pouget, J. P., Jozefowicz, M. E., Epstein, A., Tang, X., & MacDiarmid, A. G. (1991). X-ray structure of polyaniline. *Macromolecules*, 24(3), 779-789.

14. Manjunath, B. R., Venkataraman, A., & Stephen, T. (1973). The effect of moisture present in polymers on their X-ray diffraction patterns. *Journal of applied polymer science*, 17(4), 1091-1099.